BBA - Molecular Cell Research 1867 (2020) 118851

Contents lists available at ScienceDirect

BBA - Molecular Cell Research

journal homepage: www.elsevier.com/locate/bbamcr

Connexin 32 induces pro-tumorigenic features in MCF10A normal breast cells and MDA-MB-231 metastatic breast cancer cells

Asli Adak[a,1], Yagmur Ceren Unal[a,1], Simge Yucel[a], Zehra Vural[a], Fatma Basak Turan[a], Ozden Yalcin-Ozuysal[a], Engin Ozcivici[b], Gulistan Mese[a,*]

[a] Department of Molecular Biology and Genetics, Izmir Institute of Technology, Urla, Izmir, Turkey
[b] Department of Bioengineering, Izmir Institute of Technology, Urla, Izmir, Turkey

ARTICLE INFO

Keywords:
Connexin 32
Proliferation
Morphology
EMT
Breast cancer

ABSTRACT

Connexins (Cx), the basic subunit of gap junctions, play important roles in cell homeostasis, and their abnormal expression and function are associated with human hereditary diseases and cancers. In tumorigenesis, connexins were observed to have both anti-tumorigenic and pro-tumorigenic roles in a context- and stage-dependent manner. Initially, Cx26 and Cx43 were thought to be the only connexins involved in normal breast homeostasis and breast cancer. Later on, association of Cx32 expression with lymph node metastasis of breast cancer and subsequent demonstration of its expression in normal breast tissue suggested that Cx32 contributes to breast tissue homeostasis. Here, we aimed to determine the effects of Cx32 on normal breast cells, MCF10A, and on breast cancer cells, MDA-MB-231. Cx32 overexpression had profound effects on MCF10A cells, decreasing cell proliferation by increasing the doubling time of MCF10A. Furthermore, MCF10A cells acquired mesenchymal-like appearance upon Cx32 expression and had increased migration capacity and expression of both E-cadherin and vimentin. In contrast, Cx32 overexpression altered the EMT markers of MDA-MB-231 by increasing the expression of mesenchymal markers, such as slug and vimentin, and decreasing E-cadherin expression without affecting their proliferation and morphology. Our results indicate, for the first time in the literature, that Cx32 has tumor-promoting roles in MCF10A and MDA-MB-231 cells.

1. Introduction

Breast cancer is one of the most frequently observed malignant diseases among women worldwide [1] and the second most deadly cancer type after the lung cancer [2]. Even though early detection has improved clinical outcomes, its metastasis to distant organs is the major cause of breast cancer related deaths [2]. Therefore, understanding the molecular mechanisms underlying breast tumor generation and metastasis is crucial for the development of prognostic and therapeutic tools.

Several key factors, including connexins (Cx), play a role in breast cancer development and metastasis [3]. Connexins in metazoans form gap junctions that facilitate the exchange of molecules smaller than 1200 Da, such as ions, secondary messengers and metabolites between neighboring cells. In this way, they regulate tissue homeostasis, differentiation, cell growth and tissue synchronization [4–6]. There are 21 different connexin isoforms in humans [6–8], and they are expressed throughout the body in a tissue- and context-specific manner [9]. In the mammary gland, Cx26 and Cx43 are the predominant connexins, and they play a role in the proliferation and differentiation of luminal and myoepithelial cells, respectively [10–12].

In the context of cancer, initial reports have indicated that the tumor suppressor role of connexins is due to both the loss of gap junctional intercellular communication (GJIC) and decreased connexin expression in tumor samples, including breast cancer [3,7]. Recently, the pro-tumorigenic and metastatic activity of connexins were also reported in a variety of cancer types such as hepatocellular carcinoma (HCC) and breast cancer [11,13,14]. The loss of Cx26 and Cx43 expression, and therefore the loss of GJIC, in human breast cancer cell lines compared to normal mammary epithelial cells suggested their anti-tumorigenic effect [15]. The anti-tumorigenic effect of connexins on breast cancer was further supported in 3D organoid studies, in which overexpression of Cx26 and Cx43 reduced anchorage independent growth and migration while enhancing the mesenchymal to epithelial

Abbreviations: Cx, connexin; GJIC, gap junctional intercellular communication; EMT, epithelial to mesenchymal transition; HCC, hepatocellular carcinoma

* Corresponding author at: Department of Molecular Biology and Genetics, Rm D206, Izmir Institute of Technology, Urla, Izmir 35430, Turkey.
E-mail address: gulistanmese@iyte.edu.tr (G. Mese).

[1] Equal contribution.

https://doi.org/10.1016/j.bbamcr.2020.118851
Received 16 January 2020; Received in revised form 3 September 2020; Accepted 4 September 2020
Available online 09 September 2020

transition [16]. In contrast, some clinical studies reported Cx26 presence in breast cancer samples which had larger tumor size, high histological grade, increased lymphatic vessel invasion, and poorer prognosis compared to Cx26-negative tumors [17,18]. Furthermore, continued Cx26 and Cx43 expression was reported in 50% of invasive breast carcinomas, indicating their pro-tumorigenic role.

Initially, Cx26 and Cx43 were thought to be the only connexins expressed in the normal human breast. Recently, Cx32 expression was also demonstrated in normal and tumorigenic breast tissues [14,19,20]. In humans, Cx32 was initially cloned from the liver, where it contributes hepatocyte differentiation [21–23]. Then, its role in myelin sheet was shown in Schwann cells of the peripheral nervous system [12,21,24,25]. Moreover, Cx32 mutations were linked to X-linked Charcot-Marie-Tooth syndrome (CMTX1, OMIM# 302800), a peripheral sensorimotor neuropathy, suggesting its importance for human physiology [26]. Cx32 was also implicated in tumorigenesis, where Cx32 knockout mice were shown to be more prone to develop chemical- or radiation-induced liver and lung cancers compared to control animals [27,28]. Even though these studies suggested the tumor suppressor role of Cx32 [29], recent studies demonstrated its pro-tumorigenic effect in hepatocellular carcinomas (HCC) [13,30].

Cx32 expression was shown in luminal epithelial cells of mouse mammary glands during development, and its expression increased during pregnancy and lactation, implicating its involvement in mammary gland homeostasis and milk production and/or secretion [11,31]. In humans, Cx32 expression was detected in the lymph node metastasis of breast cancers [14,19,32] which was followed by the demonstration of Cx32 expression in luminal epithelial cells of human breasts [20]. As the role of Cx32 is not known in breast tissue and cancer, we aimed to investigate the effect of Cx32 on the non-tumorigenic mammary cell line, MCF10A, and metastatic breast cancer cell line, MDA-MB-231.

2. Materials and methods

2.1. Cell culture

MDA-MB-231 (ATCC® HTB-26) and 293T cells were cultured in high glucose Dulbecco's Modified Eagle Medium (DMEM) (GIBCO, Cat# 41966029) supplemented with 10% Fetal Bovine Serum (FBS; GIBCO, 16000044) and 1% Penicillin/Streptomycin (P/S; GIBCO, 15140122). MCF10A cells (ATCC® CRL-10317) were cultured in DMEM/F-12 medium (GIBCO, 31330038), which was supplemented with 5% Donor Horse Serum (DHS; Biological Industries, 04-004-1B), 1% Penicillin/Streptomycin, 20 ng/mL EGF (Sigma, E9644), 0.5 μg/mL Hydrocortisone (Sigma, H0888), 100 ng/mL Cholera Toxin (Sigma, C8052) and 10 μg/mL Insulin (Sigma, I1882). NIH3T3 cells were cultured in DMEM high glucose medium supplemented with 10% Newborn Calf Serum (NBCS) (Biological Industries, 04–102-1A) and 1% P/S. All cells were kept in a humidified chamber with 5% CO_2 at 37 °C.

2.2. Transfection

For overexpression studies, 4×10^5 MDA-MB-231 cells/well were seeded in 6-well plates and incubated for 48 h. 5×10^5 MCF10A cells/well were plated in 6-well plates and incubated for 24 h. MDA-MB-231 and MCF10A were transfected with pIRES2-EGFP2 and pIRES2-EGFP2-Cx32 using Fugene HD (Promega, E2311) according to the manufacturer's protocol.

For shRNA silencing studies, 2.5×10^5 MCF10A and MCF10A-Cx32 cells/well were plated in 6-well plates for 48 h. shRNA-Cx32 (GE Dharmacon, RHS4531-EG2705-V2LHS_257226 (shCx32#3)) and scrambled shRNA (GE Dharmacon, RHS4430–200189226-V2LHS_177060) as control were transfected using Fugene HD according to the manufacturer's manual. 48 h after transfection, cells were collected for Western blot analysis.

2.3. Virus production and titration

$3.5–4.5 \times 10^6$ 293T cells were plated in 10 cm plates for 24 h. Then, cells were transfected with the lentiviral plasmids: pLenti-GIII-CMV-GFP-2A-Puro (pLenti-GFP) or pLenti-GIII-CMV-GFP-2A-Puro-Cx32 (pLenti-Cx32; ABMGOOD, LV169789) with packaging vector (pCMVdR8.74) and envelope vector (pMD2.VSVG) using Fugene HD according to the manufacturer's protocol. 48 and 72 h after transfection, the viruses were collected and stored at −80 °C [33].

For virus titer, 2×10^5 NIH3T3 cells/well were cultured in 6-well plates for 24 h. Cells were infected with serial dilutions of viruses containing 8 μg/mL polybrene. After centrifugation at 2500 rpm for 2 h at 32 °C, fresh medium was added to plates. 48 h after infection, the cells were transferred to 10 cm plates having selection medium with 2 μg/mL puromycin. After selection was complete, the plates were washed with 1× PBS and were then incubated with 0.5% Crystal Violet staining solution for 10 min on a shaker at room temperature. Following washing steps with 1× PBS, the colonies on the plates were counted and virus preps with similar titer were used for cell infections.

2.4. Infection

3.5×10^5 MDA-MB-231 cells/well and 2.5×10^5 MCF10A cells/well were plated in 6-well plates for 24 h. Then, cells were infected with pLenti-GFP and pLenti-Cx32 viruses by centrifugation for 2 h at 2500 rpm and 32 °C. 48 h later, cells were transferred to 10 cm plates with selection medium containing 2 μg/mL puromycin until all cells in mock condition were dead.

2.5. Immunostaining and fluorescence imaging

MDA-MB-231 and MCF10A cells were grown on coverslips in 6-well plates for 48 h and 24 h, respectively. Cells were fixed with 4% Paraformaldehyde (PFA) in 1× Phosphate-Buffered Saline (PBS) for 20 min, permeabilized with 0.1% TritonX-100/PBS for 15 min and blocked with 3% BSA in 0.1% TritonX-100/PBS for 30 min at room temperature. 1:200 dilution of polyclonal rabbit anti-Cx32 antibody (Invitrogen, 34–5700) incubation was performed for 1 h at room temperature (RT) or overnight at 4 °C. Then, cells were incubated with Alexa555-conjugated goat anti-rabbit secondary antibody (Invitrogen, A21428) with 1:200 dilution and 4′,6-Diamidino-2-Phenylindole (DAPI) (Sigma, D9542) with 1:1000 dilution for 1 h at room temperature in the dark. After the coverslips were mounted on slides, the images were taken with the Olympus fluorescent microscope [34].

For cell morphology analysis, cells grown on coverslips were treated as above and then immunostained for actin with Alexa Fluor-488 Phalloidin (1:500 dilution, Invitrogen, A12379) and DAPI for 1 h at room temperature. Then the coverslips were mounted by mounting medium (Ibidi, 50001) on slides and the images were taken with the Olympus fluorescent microscope. The circularity index of each cell in the images was determined with ImageJ (NIH, USA) that gives ratios between 0 and 1, where 1 represents a perfect circle.

2.6. qRT-PCR analysis

48 h and 24 h post transfection of MDA-MB-231 and MCF10A cells, they were flash frozen, respectively. Stable MDA-MB-231 and MCF10A cells were flash frozen 48 h after plating. By using PureLink® RNA Mini Kit (Lifetech, 12183018A), the total RNA was isolated from cells by following the manufacturer's protocol. After the determination of RNA concentration, cDNA was synthesized using 1 μg total RNA with the cDNA Synthesis Kit (ThermoFisher, K1622) following the manufacturer's protocol. qRT-PCR was performed with the following primer pairs: Cx32 5′-GGCACAAGGTCCACATCTCA-3′, 5′-GCATAGCCAGGGTAGAGCAG-3′; GAPDH 5′-GAAGGTGAAGGTCGGAGTCA-3′, 5′-AATGAAGGGGTCATTGATGG-3′; E-cadherin 5′-CAGCACGTACACAGCCC

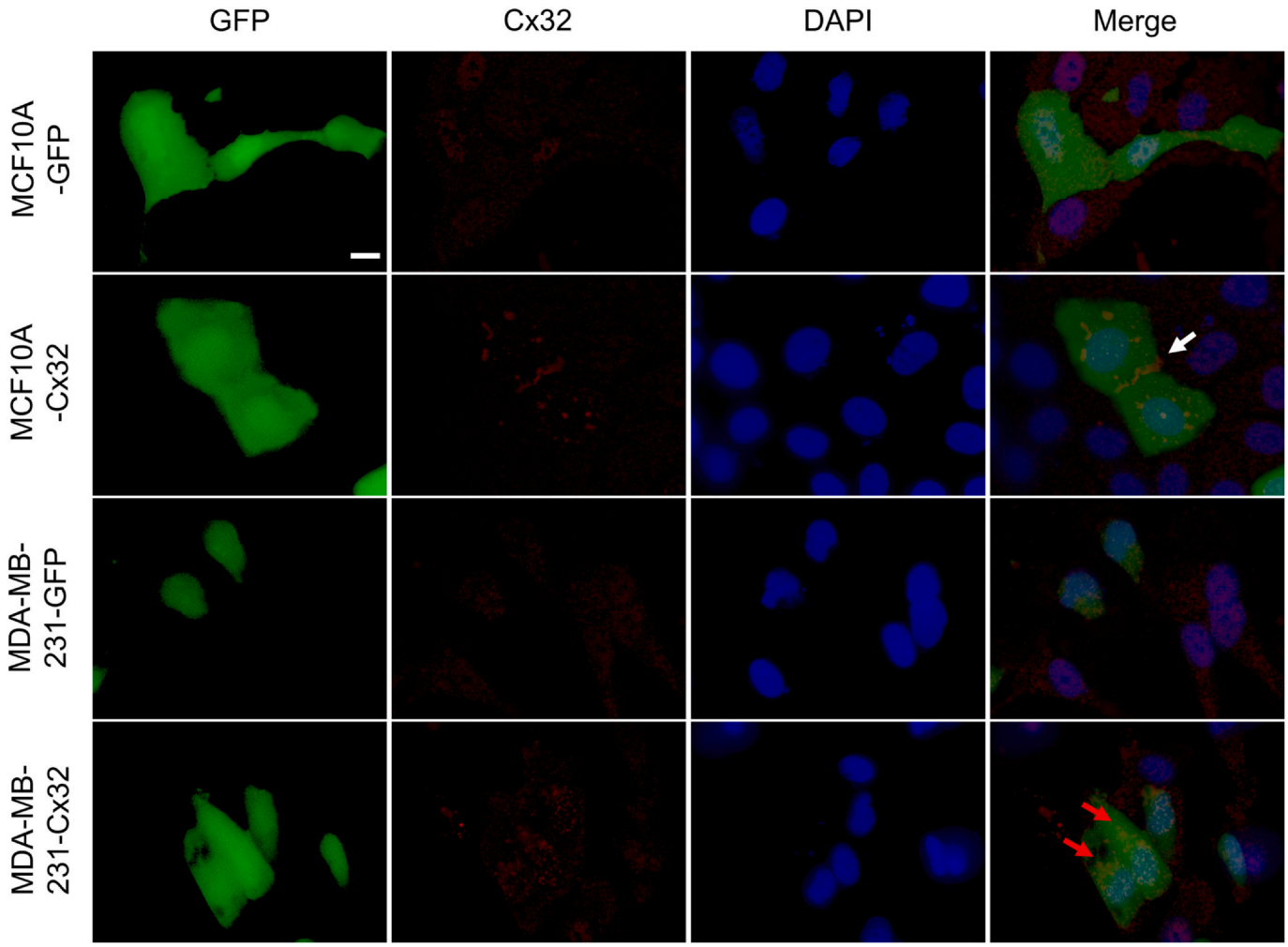

Fig. 1. Cx32 overexpression resulted in differential localization of protein in MCF10A and MDA-MB-231 cells. When MCF10A and MDA-MB-231 cells were transiently transfected with control and Cx32 containing constructs, it altered Cx32 cellular localization. Green is for EGFP, red is for Cx32 and blue represents the nucleus. White arrow points the gap junction plaques between MCF10A-Cx32 cells and red arrows demonstrate Cx32 cellular localization in MDA-MB-231-Cx32. Scale bar is 10 μm.

TAA-3′, 5′-GGTATGGGGGCGTTGTCATT-3′; vimentin 5′-GCTAACCAA CGACAAAGCCC-3′, 5′-CGTTCAAGGTCAAGACGTGC-3′; slug 5′-CTCCT CATCTTTGGGGCGAG-3′, 5′-TTCAATGGCATGGGGGTCTG-3′. Each gene's expression data were normalized to endogenous control gene GAPDH and relative mRNA values were presented as the mean ± S.D. of three independent experiments by normalizing Cx32 data to GFP samples.

2.7. Western blot analysis

Cells were grown in 6-well plates to 80–90% confluency and were scraped off with 3 mL ice-cold lysis buffer (100 mM Tris-HCl, 1 mM EDTA, 0.1% Triton X) on ice. They were then centrifuged at 14000 *g* for 20 min at 4 °C, and supernatant was collected. After the determination of protein concentrations using Bradford reagent, cell lysates were then resolved in 10% SDS-PAGE gel and transferred to the PVDF membrane. After blocking with 5% milk powder in 1× TBS-T, membranes were incubated overnight at 4 °C with 1:500 dilution of primary antibodies against Cx32 (Invitrogen, 71–0600) and gamma-tubulin (Sigma, T6557) or beta-actin (ABCAM, ab8227) followed by incubation with 1:500 dilutions of secondary anti-rabbit (Invitrogen, 31460) or anti-mouse (Dako, P0447) antibodies conjugated to horseradish peroxidase. The membrane was visualized by chemiluminescence using the Vilber Fusion SL Imaging System. The band intensities for each protein were quantified with the Gel Analysis tool of ImageJ and normalized to control gamma-tubulin intensity. Then, the data were presented by normalizing the values for Cx32 samples with respect to GFP control cells.

2.8. MTT assay for cell viability

After seeding of 2 × 10^3 MCF10A and MDA-MB-231 cells/well in 48-well plates, cell viability was measured on day 1, 4, 7 and 10. On each day, cells were incubated in a medium containing 10% 3-(4,5-Dimethylthiazol-2-yl)-2,5-diphenyltetrazolium bromide (MTT) solution for 4 h in the incubator. After the removal of MTT, dimethyl sulfoxide (DMSO) was added to dissolve the tetrazolium salts for colorimetric measurement of the samples with spectrophotometer at 570 nm and 650 nm. All data were normalized to day 1 of each sample for comparison of GFP control and Cx32-overexpressing cells.

2.9. Trypan blue counting

1 × 10^4 cells/well were cultured in a 12-well plate for 7 to 9 days. On each day, cells were counted with trypan blue staining and haemocytometer in duplicates. The experiment was repeated three times, and doubling time was calculated by analyzing cell numbers obtained at their log phases with the formula: Dt = ln2/μ where μ = ln(Total

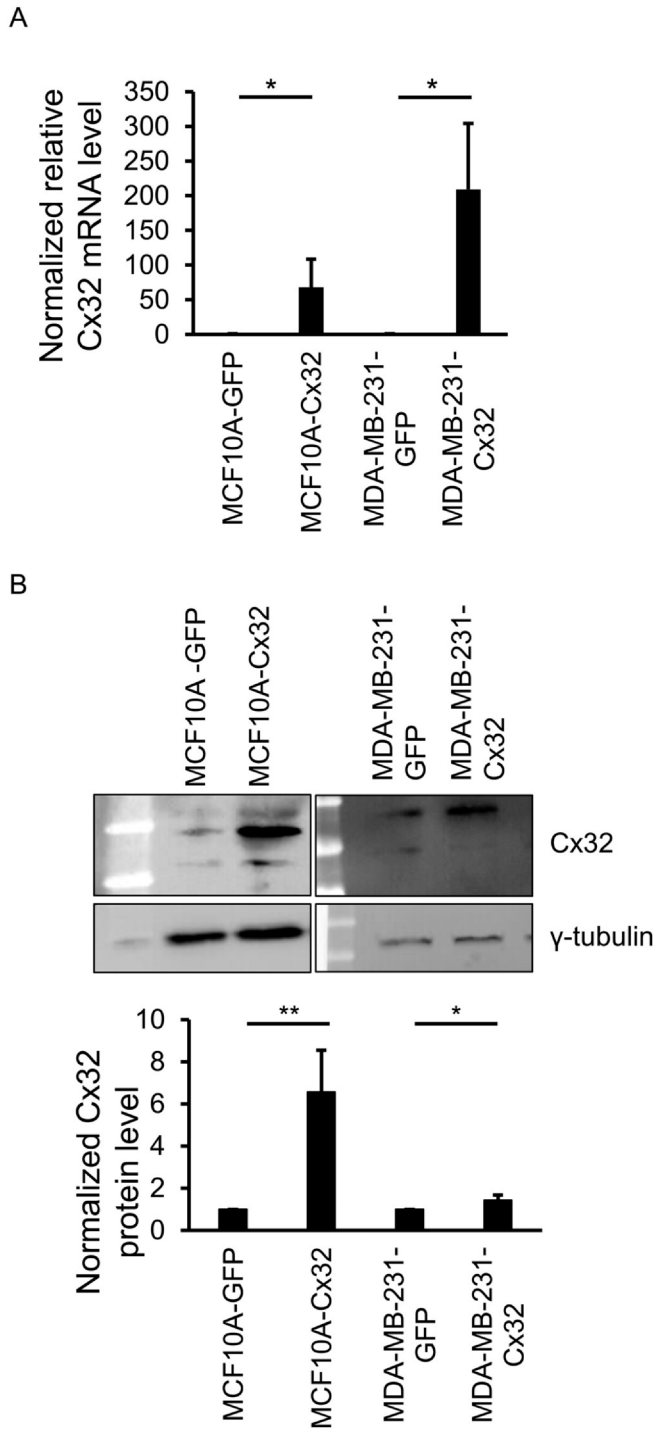

Fig. 2. Verification of Cx32 overexpression upon viral infection in MCF10A and MDA-MB-231 cells. A) Semi-quantitative RT-PCR analysis for Cx32 mRNA level comparison in GFP and Cx32-overexpressing cells (*$p < 0.05$; $n = 3$). B) Representative images for Cx32 and γ-tubulin protein detection and comparison of Cx32 protein level normalized to γ-tubulin in MCF10A-GFP and MDA-MB-231 cells (*$p < 0.05$ and ** $p < 0.01$; $n = 3$). All data are presented as mean ± S.D. by normalizing Cx32 values with respect to GFP controls.

number of cells counted at last day of log phase)/ln(Total number of cells counted at initial day of log phase) [35].

2.10. PI staining for cell cycle analysis

48 h after culturing 4 × 10^5 MCF10A and MDA-MB-231 cells/well in 6-well plates, cells were washed with 1× PBS. After trypsinization, cells were centrifuged for 10 min at 1200 rpm. The cell pellets were incubated on ice and were re-suspended in cold 1× PBS. Then, cells were fixed with ice-cold 100% EtOH at −20 °C for at least overnight. Subsequently, cells were centrifuged at 1500 rpm for 10 min and followed by another centrifugation at 2000 rpm for 1 min. The pellets were re-suspended in 1× PBS, and cells were centrifuged at 1500 rpm for 10 min at 4 °C. Then, the pellets were re-suspended in 0.1% TritonX-100/PBS containing 200 μg/mL RNase A and were incubated at 37 °C for 30 min. After the addition of Propidium Iodide (PI; Invitrogen, P1304MP), cells were incubated in the dark for 15 min and analyzed using the FACS Canto instrument (BD Biosciences, CA, USA).

2.11. Wound healing assay

48 h after plating 2 × 10^6 MCF10A and 2.5 × 10^5 MDA-MB-231 cells/well in 12-well plate, cells were washed with 1× PBS. Then, cells were incubated with a serum free medium containing 10 μg/mL Mitomycin C at 37 °C for 2 h. After scratching with a 10 μl pipette tip, cells were washed with 1× PBS and kept in a starvation medium, 1.3% DHS containing medium for MCF10A and 1% FBS containing medium for MDA-MB-231 cells. Time-lapse images of at least three positions per well were taken using Leica SP8 under 37 °C and 5% CO_2 conditions for 24–48 h. Images were analyzed by determining the open area percentages for each position using MRI Wound Healing Tool macro on ImageJ [36].

2.12. Statistical analysis

Data are presented as the mean ± standard deviation (S.D.) of at least 3 biological replicates. Statistical differences between GFP and Cx32 expressing cells were compared with the Student's *t*-test, and differences were considered significant when $p < 0.05$.

3. Results

3.1. Cx32 localization showed different patterns in MCF10A and MDA-MB-231 cells

In order to determine the effect of human Cx32 (Cx32) on MCF10A normal breast and MDA-MB-231 invasive breast cancer cells, cells were first transiently transfected with either control pIRES2-EGFP2 or pIRES2-EGFP2-Cx32 vectors. Then, the expression and localization of Cx32 in cells were examined with immunostaining and fluorescence imaging (Fig. 1). Transient expression of Cx32 in MCF10A resulted in the localization of proteins to the plasma membrane, where they could form gap junction plaques between adjacent cells (white arrow in the merge image of MCF10A-Cx32) compared to GFP expressing control cells. Additionally, overexpression of Cx32 in MDA-MB-231 cells caused localization of the protein around the nucleus compared to dispersed distribution in GFP-expressing control cells (red arrows in the merge image of MDA-MB-231-Cx32), suggesting that Cx32 overexpression caused differential localization of the protein in normal breast cells and invasive breast cancer cells.

3.2. Cx32 over-expression had distinct effects on the viability, cell cycle and growth of normal breast and breast cancer cells

Transient transfection of cells hindered the long-term studies due to low transfection efficiency. For that reason, stable Cx32 overexpression was obtained by infecting cells with pLenti-GFP and pLenti-Cx32 viruses followed by selection with puromycin antibiotics. Cx32 overexpression in stable cell lines was confirmed by semi-quantitative RT-PCR and Western blot analysis (Fig. 2). At the mRNA level, Cx32 expression increased 68 fold in MCF10A cells ($p < 0.05$) and 209 fold in MDA-MB-231 cells ($p < 0.05$) with respect to their GFP control

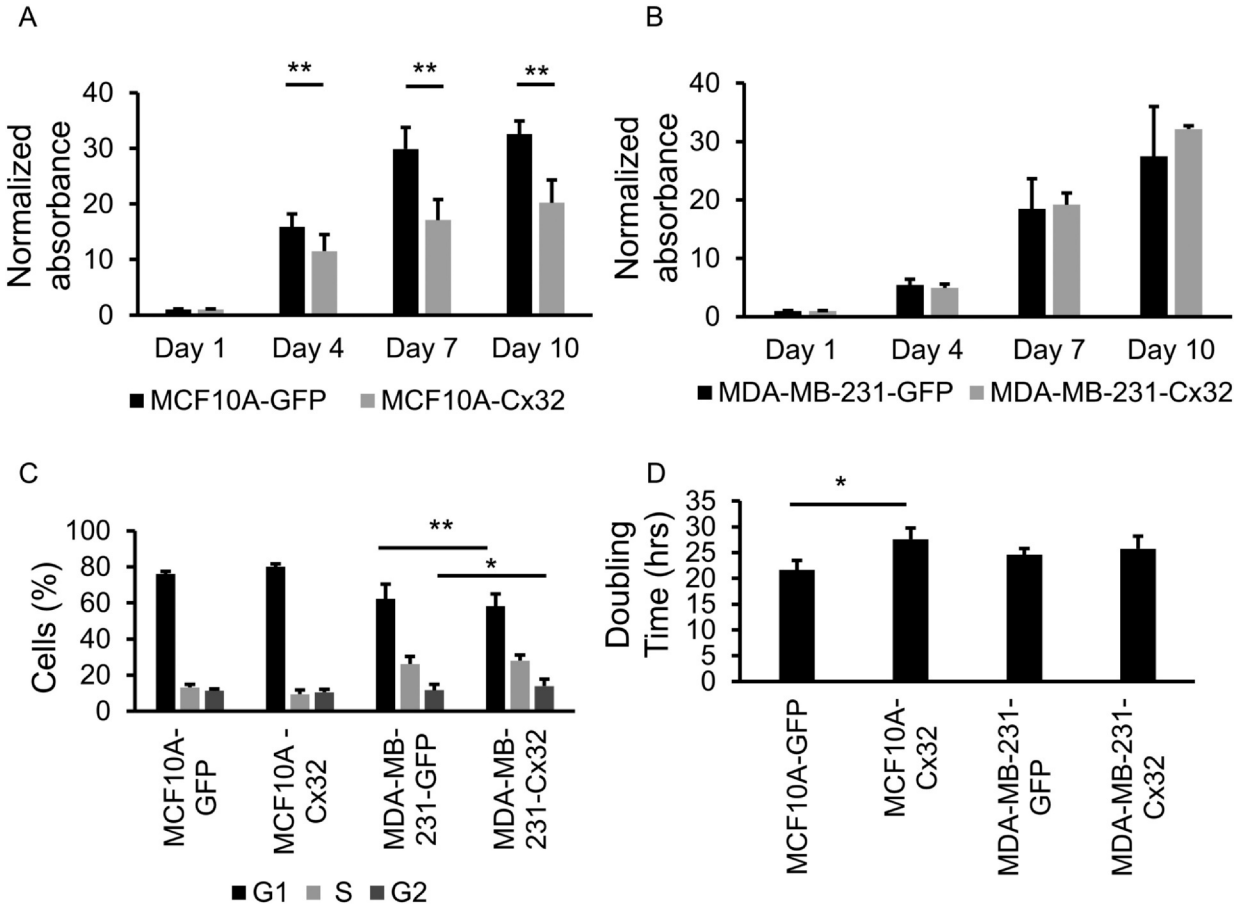

Fig. 3. Cx32 overexpression delayed cell proliferation and increased doubling time in MCF10A cells with no effect on MDA-MB-231 cells. A) Comparison of normalized absorbance in day 1, day 4, day 7 and day 10 in normal breast cell line MCF10A (**p < 0.01; n = 3) suggested a decrease in the viability of cells due to Cx32 overexpression in MTT analysis. B) Cx32 overexpression did not interfere with the viability of MDA-MB-231 breast cancer cells assessed by MTT assay. C) Evaluation of cell percentages found in G_1, S and G_2 cell cycle phases in MCF10A and MDA-MB-231 cells by PI staining demonstrated differential effect of Cx32 on cell cycle (*p < 0.05 and ** $p < 0.01$; $n = 4$). D) Growth curve of cells was generated for 7–9 days and doubling time was compared between GFP- and Cx32-expressing MCF10A and MDA-MB-231 cells where the doubling time for MCF10A cells increased upon Cx32 overexpression (*$p = 0.05$; $n = 3$). All data are presented as mean ± S.D.

Table 1
Doubling times and times spent in each phase of cell cycle.

Cells	Doubling time (h)	G_1 time (h)	S time (h)	G_2 time (h)
MCF10A-GFP	21.6 ± 1.8	16.5 ± 1.8	2.8 ± 0.9	2.5 ± 0.7
MCF10A-Cx32	27.6 ± 2.2*	22.1 ± 1.9**	2.6 ± 0.9	2.9 ± 1.1
MDA-MB-231-GFP	24.6 ± 1.2	15.3 ± 0.33	6.4 ± 0.4	2.9 ± 0.3
MDA-MB-231-Cx32	25.8 ± 2.4	15 ± 0.4	7.2 ± 0.6	3.6 ± 0.4*

All data is presented as mean ± S.D.
* $p < 0.05$.
** $p < 0.01$.

infections (Fig. 2A). In parallel with mRNA expression, Cx32 protein levels were increased 6.5 fold ($p < 0.01$) in MCF10A cells and 1.4 fold ($p < 0.05$) in MDA-MB-231 cells (Fig. 2B).

During the cell culture, we observed a growth delay in MCF10-Cx32 cells, so we next determined Cx32's effect on cellular viability on the 1st, 4th, 7th and 10th days with MTT assay. Absorbance of samples on each day was normalized to absorbance at day 1 and was compared between GFP and Cx32-expressing cells. For MCF10A cells, the viability of cells expressing Cx32 significantly decreased compared to control cells starting from day 4, and this difference was maintained until day 10 (Fig. 3A, $p < 0.01$). On the other hand, Cx32 overexpression did not interfere with the viability of MDA-MB-231 cells, as there was no statistically significant difference in the normalized absorbance between GFP and Cx32-expressing cells (Fig. 3B). This suggested that Cx32 overexpression reduced the proliferation of normal breast cells without changing that of invasive breast cancer cells.

Next, to examine if the reduced proliferation in MCF10A-Cx32 cells was due to alteration in cell cycle phases, propidium iodide (PI) staining followed by flow cytometry was used to compare the percentages of cells in G_1, S and G_2 phases between GFP and Cx32-expressing cells (Fig. 3C). In contrast to the alteration in the viability of MCF10A-Cx32 cells, no significant changes were observed in the percentages of cells in G_1, S and G_2 phases with respect to MCF10A-GFP cells, suggesting that the reduced proliferation in MCF10A-Cx32 cells was not due to the alteration of percentages of cells in different phases of the cell cycle. On the other hand, even though there was no change in the viability of MDA-MB-231 cells in MTT assay, the percentages of cells in G_1 decreased in Cx32-overexpressing cells compared to GFP control cells ($p < 0.05$), while the percentages of cells in G_2 increased upon Cx32 overexpression ($p < 0.01$) (Fig. 3C).

3.3. Cx32 extended doubling time of MCF10A cells

It was previously shown that Cx37 reduced the proliferation of Rin (rat insulinoma) cells by altering the duration of cell cycle phases and increasing the doubling time of cells from 2 days to 9 days [37].

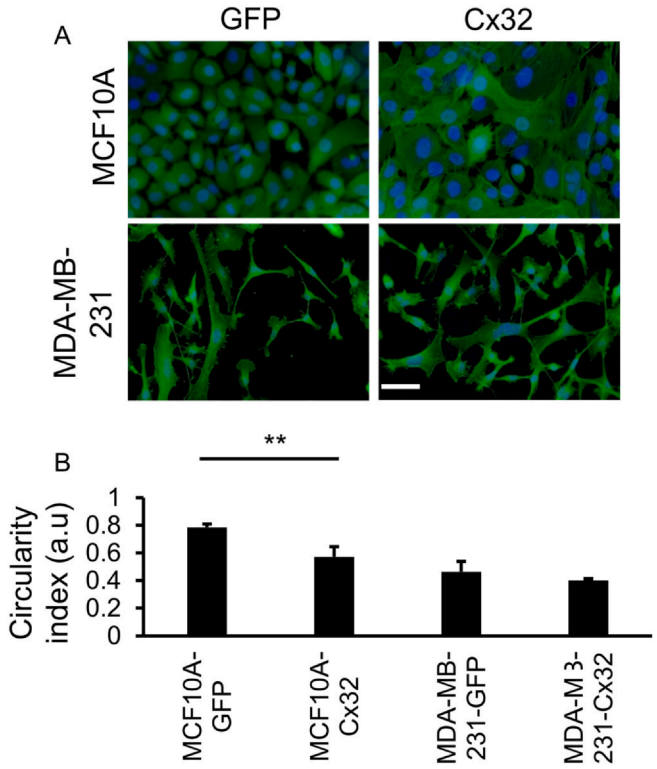

Fig. 4. MCF10A-Cx32 cells acquired mesenchymal-like morphology compared to MCF10A-GFP. Cell morphology in GFP and Cx32 overexpressing MCF10A cells and MDA-MB-231 cells were examined by (A) phalloidin staining of actin cytoskeleton (scale bar is 50 μm) and (B) determination of cell circularity index (**$p < 0.01$; n = 3). Cx32 induced a more elongated shape in MCF10A cells without changing the MDA-MB-231 cell shape. All data are presented as mean ± S.D.

Therefore, it was assumed that the decrease in the cell viability of MCF10A-Cx32 cells might be due to the alteration of the cells' doubling time; thus, MCF10A and MDA-MB-231 cells were counted using trypan blue staining and haemocytometer every day for 7–9 days for the assessment of cell growth. Based on the growth curves, the doubling time for MCF10A-GFP cells was determined to be 21.6 (± 1.8) h while that for MCF10A-Cx32 cells significantly increased to 27.6 (± 2.2) h (Fig. 3D, $p < 0.05$). Then, the times that were spent in each cell cycle phases were determined using the calculated doubling times. Based on these, the time that MCF 10A-Cx32 cells spent in G_1 increased from 16.5 h to 22 h ($p < 0.01$) compared to control cells (Table 1). This increase in doubling time due to the extension of G_1 phase for MCF10A-Cx32 cells could contribute to the reduction observed in the viability of cells in MTT assays.

On the other hand, the doubling time did not change for MDA-MB-231 cells consistent with the MTT results, which were 24.6 (± 1.2) and 25.8 (± 2.4) h for GFP and Cx32-overexpressing cells, respectively (Fig. 3D, $p = 0.49$). However, Cx32-overexpressing MDA-MB-231 cells spent 24% ($p < 0.05$) more time in G_2 phase compared to control cells in parallel with the MTT analysis (Table 1).

3.4. Cx32 resulted in mesenchymal-like morphology in MCF10A cells

When the cells were observed under the microscope during culturing, morphological differences in MCF10A cells overexpressing Cx32 were noticed compared to control GFP cells, in addition to reduced proliferation. In order to verify this, immunostaining for actin cytoskeleton was performed to examine the cellular morphology by assessing the circularity index using ImageJ (NIH) [38,39]. Florescent images suggested that Cx32 expressing cells were more elongated; that is, they had mesenchymal-like appearance compared to epithelial features of GFP control cells (Fig. 4A, top panel). This morphological change was further verified with a 27% reduction in the circularity index of MCF10A-Cx32 cells with respect to MCF10A-GFP cells (Fig. 4B, $p < 0.01$). In contrast to MCF10A cells, Cx32 overexpression in MDA-MB-231 cells did not cause any changes in either cell morphology or circularity index, as shown by immunostaining images or ImageJ analysis, respectively (Fig. 4A bottom panel and Fig. 4B).

3.5. Cx32 increased the migration of MCF10A cells

After observing morphological changes in MCF10A-Cx32 cells, we aimed to determine if Cx32 alters MCF10A and MDA-MB-231 cells' migration potential using wound healing assay. 48 h after plating, we treated cells with mitomycin C for 2 h before the scratch to stop cell proliferation and then monitored them until the closure of the gap by taking images every hour. Cx32-expressing MCF10A cells started to close the gap earlier than their control counterparts did, as observed in images at 10 and 20 h (Fig. 5A). Percentages of the open area (area within the yellow trace) at 5, 10, 15, 20 and 25 h demonstrated that MCF10A-Cx32 cells closed the gap faster than MCF10A-GFP cells from the 5th hour until the end of the experiments (Fig. 5B, $p < 0.01$). This implicated that Cx32 overexpression increased the migration potential of MCF10A normal breast cells by acquiring a mesenchymal-like morphology. In parallel with morphological assessment, Cx32 overexpression did not interfere with the migration potential of MDA-MB-231 cells, as no difference was observed neither in time-lapse images (Fig. 5C) nor in the comparison of percentages of open areas (Fig. 5D) between Cx32 and GFP-expressing cells.

3.6. Cx32 altered the expression of EMT markers in MCF10A and MDA-MB-231 cells

In accordance with changes in morphological appearances and increased migration of MCF10A-Cx32 cells, expression of epithelial to mesenchymal (EMT) markers was investigated in MCF10A and MDA-MB-231 cells. We compared the expression of the epithelial marker E-cadherin and the mesenchymal markers vimentin and slug between GFP and Cx32 overexpressing cells with semi-quantitative RT-PCR and Western blot analysis (Figs. 6, 7 and 8). Even though Cx32 overexpression in MCF10A cells did not alter E-cadherin, vimentin and slug relative mRNA levels (Fig. 6A), the protein levels of E-cadherin and vimentin increased by 2.4 fold ($p < 0.01$) and 2.1 fold ($p < 0.01$), respectively (Fig. 6B).

To verify that Cx32 altered the EMT marker expression, we transiently silenced Cx32 in both MCF10A cells and stable MCF10-Cx32 cells and examined E-cadherin and vimentin protein expression (Fig. 7). In MCF10A cells, Cx32 protein expression decreased by ~50% ($p < 0.01$) in shRNA-Cx32 transfected cells compared to cells with control shRNA. This decrease was accompanied by a 43% reduction ($p < 0.05$) in E-cadherin level without no change in vimentin between control and shRNA-Cx32 transfected cells (Fig. 7A). Then, we wanted to determine if Cx32 silencing would alter E-cadherin and vimentin expression in MCF10A-Cx32 stable cell lines. shRNA-Cx32 reduced the Cx32 level by 31% ($p < 0.01$) and E-cadherin level by 34% ($p < 0.0005$) in MCF10A-Cx32 cells (Fig. 7B) without interfering with vimentin level, suggesting that Cx32 affects the E-cadherin levels in MCF10A cells.

In MDA-MB-231 cells, relative E-cadherin mRNA expression was reduced by 53% ($p < 0.005$) and vimentin ($p < 0.001$) and slug ($p < 0.05$) mRNA increased by 1.3 fold (Fig. 8A). In accordance with mRNA expression, Cx32 overexpression caused a %58 reduction in E-cadherin protein level ($p < 0.05$), but no significant change was observed in vimentin and slug protein levels between Cx32-overexpressing cells and GFP control cells (Fig. 8B). These results suggest that Cx32 induces mesenchymal features in both MCF10A and MDA-

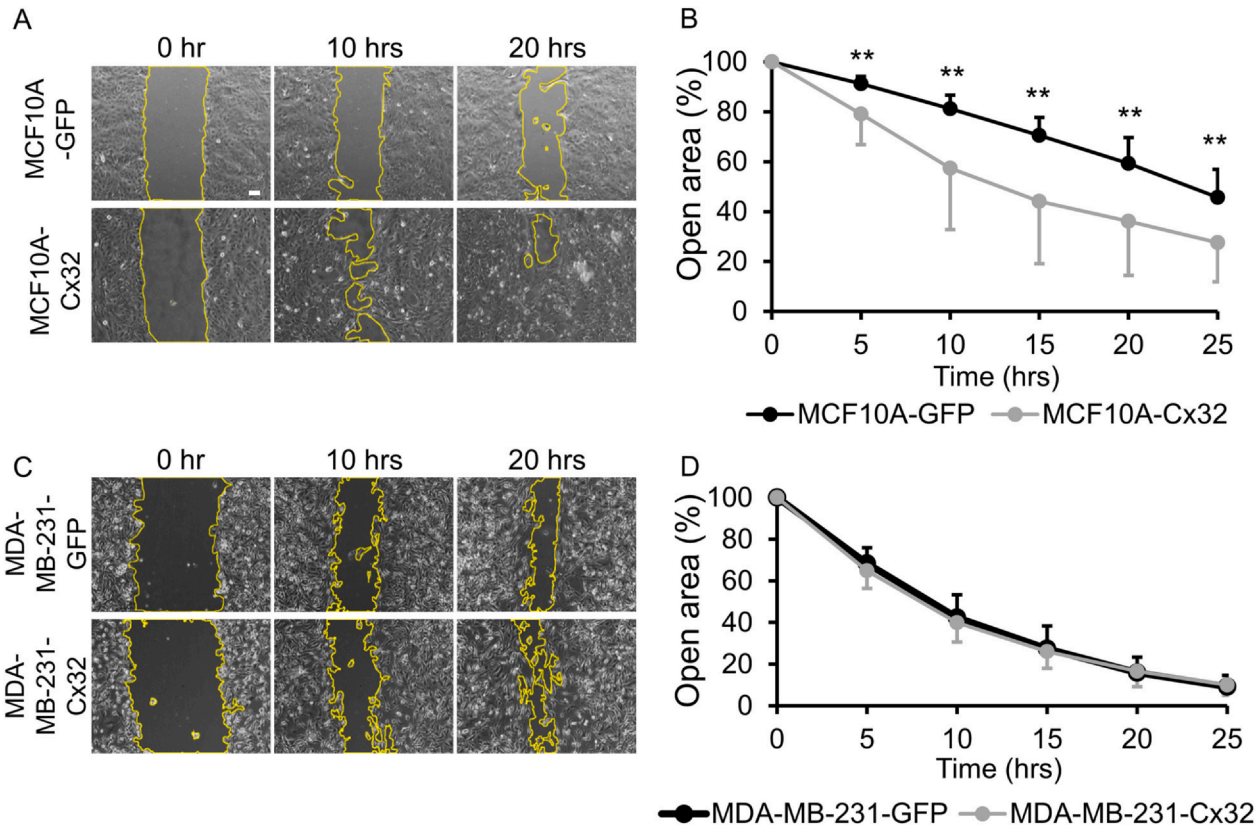

Fig. 5. Cx32 increased migration of MCF10A cells without affecting that of MDA-MB-231 cells. A) Representative images of MCF10A cells at 0, 10 and 20 h and B) Comparison of percentage of open area (areas within the yellow lines) between MCF10A-GFP and MCF10A-Cx32 cells suggested an increase in migration of MCF10A cells upon Cx32 overexpression (**$p < 0.01$; $n = 3$). C) Representative images of MDA-MB-231 cells at 0, 10 and 20 h and D) Comparison of percentage of open area (areas within the yellow lines) between MDA-MB-231-GFP and MDA-MB-231-Cx32 cells showed no difference in the migration. Scale bar is 50 μm and all data are presented as mean ± S.D.

MB-231 cells.

4. Discussion

Connexin 32, the major connexin of the liver and the Schwann cells of the peripheral nervous system, was recently shown to be expressed in normal breast tissue [20]. Furthermore, elevated Cx32 expression was observed in the metastasis of breast cancer cells to lymph nodes, implicating the involvement of Cx32 in mammary homeostasis and breast cancer tumorigenesis [14,32]. Here we investigated the effect of Cx32 on the normal breast cell line, MCF10A, and the metastatic breast cancer cell line, MDA-MB-231. We demonstrated that Cx32 resulted in reduced proliferation of MCF10A cells by extending the duration of G_1 phase and thus increasing their doubling time. Further, MCF10A cells acquired a mesenchymal-like morphology accompanied by increased migration upon Cx32 overexpression. Finally, increase in the level of vimentin protein together with morphological and motility changes suggested that Cx32 might induce a mesenchymal state in MCF10A cells. Meanwhile, Cx32 overexpression in MDA-MB-231 cells decreased the mRNA and protein expression of E-cadherin while increasing vimentin and slug at mRNA levels without altering their protein expression. These results suggest that Cx32 might have a pro-tumorigenic effect in MCF10A and MDA-MB-231 cells.

Connexins can have either pro- or anti-tumorigenic effects in cancer depending on tissue type and cancer stage. The tumor-suppressing roles of Cx26 and Cx43 were demonstrated in both patient samples and cell lines due to reduced Cx26 and Cx43 expression and gap junctional intercellular communication (GJIC) [16]. In contrast, increased expression of Cx26 and Cx43 was correlated with brain metastasis of both melanoma and breast cancers, demonstrating their pro-tumorigenic features in cancer [40]. The involvement of Cx32 in tumorigenesis can also be pro- and anti-tumorigenic. For example, induction by X-ray radiation made Cx32 knockout mice more susceptible to liver and lung cancers than the controls, suggesting its tumor-suppressor roles [27,28]. Furthermore, Cx32-dependent GJIC in Huh7 hepatoma cells showed tumor-suppressor effect while cytoplasmic Cx32 accumulation promoted their proliferation, invasion and metastasis [13], indicating the differential effect of Cx32 on tumorigenesis based on cellular localization. As stated above, the effects of connexins on tumorigenesis are context-dependent. In this study, we observed that even though Cx32 overexpression decreased the proliferation of MCF10A, which might suggest its anti-tumorigenic effect, changes in morphology, migration and vimentin expression supported the pro-tumorigenic features.

Connexins interfere with cell cycle progression. For example, Cx43 was shown to inhibit cell proliferation and to prevent G1/S transition by inhibiting S phase kinase-associated protein 2 (Skp2) [41]. Along this line, Cx50 was shown to directly interact with and regulate Skp2 to induce cell cycle arrest in lens cells [42]. Further, Cx37 in rat insulinoma cells were shown to reduce cell proliferation by slowing cell cycle progression in these cells [37]. Similarly, Cx32 induced cell cycle arrest in gastric cancer cells and inhibited proliferation [43]. Here we also observed a decrease in proliferation of MCF10A cells due to Cx32 overexpression which can be attributed to the extension of the G_1 phase and hence the increase in the doubling time of MCF10A cells. However, the molecular mechanisms leading to the extension of the cell cycle in breast cells due to Cx32 overexpression remains elusive.

There are numerous studies on the role of connexins in cell morphology and migration [44–46]. Cx43 knockout impaired directionality and reduced speed in cardiac neural crest cells in addition to alteration

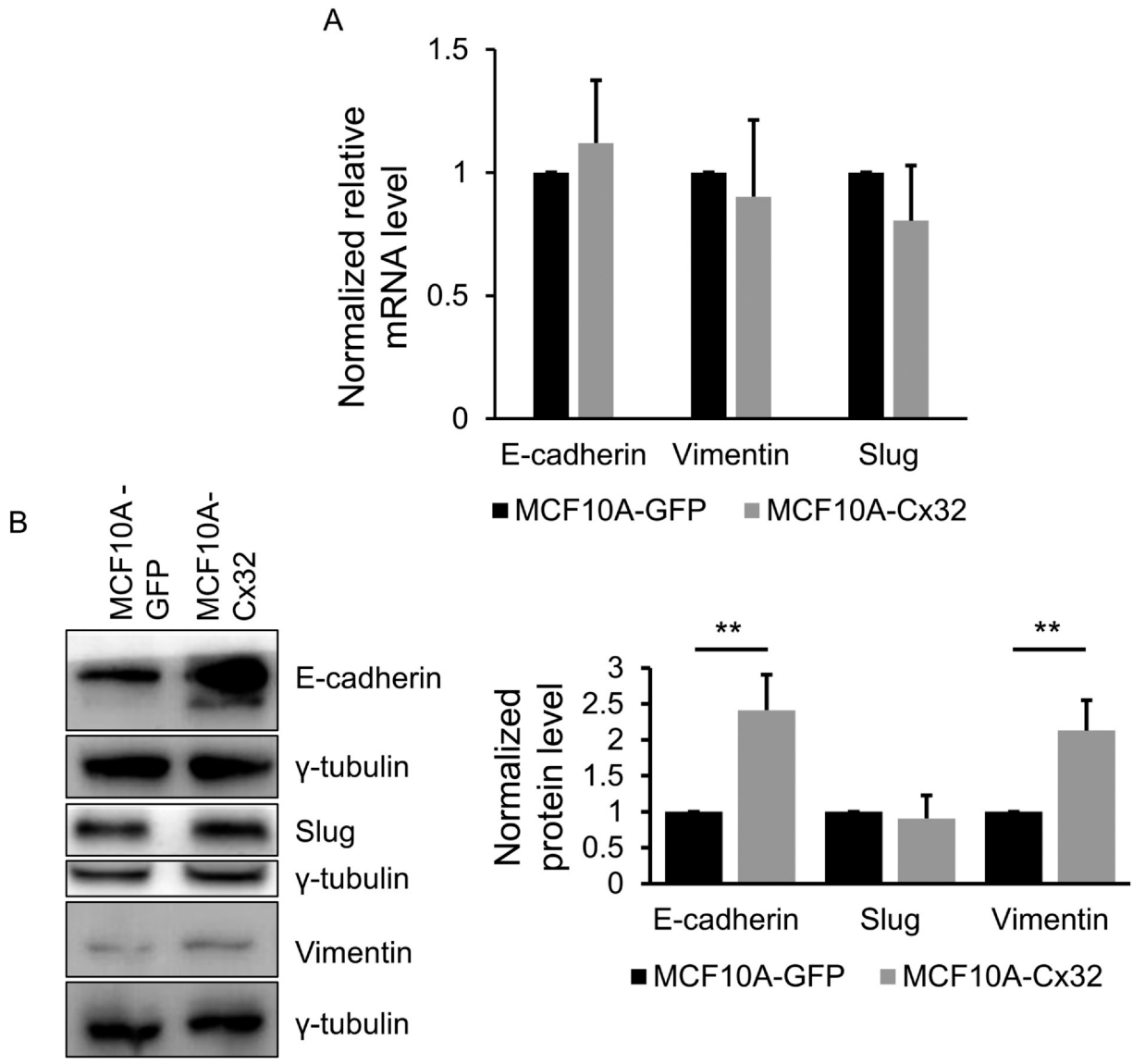

Fig. 6. Cx32 overexpression increased E-cadherin and vimentin expression in MCF10A cells. Relative mRNA (A) and protein (B) levels of epithelial marker E-cadherin and mesenchymal markers vimentin, and slug in MCF10A suggested that Cx32 induced mesenchymal features in these cells (**$p < 0.01$, $n = 4$). All data are presented as mean ± S.D. by normalizing Cx32 values with respect to GFP controls.

in actin cytoskeleton [47]. Similarly, neuronal migration was impaired in embryonic Cx43 knockout mice during development [44]. In connection with this, high Cx43 expression was correlated with increased migration capacity compared to low Cx43 levels in C6 glioma cells, which was reversed by Cx43 downregulation [45]. In a recent study, Cx43 downregulation increased cell circularity and decreased neural cell migration in *Xenopus* leavis and Cx43-20k isoform was shown to regulate cell morphology and migration by directly regulating N-cadherin expression [39]. In breast cancer, decreased Cx43 expression reduced the motility in MDA-MB-231 and HS578T cells without affecting their morphology [48]. Silencing of Cx43 in MCF10A cells resulted in lack of polarity, disorganized movement and variation in cell-cell adhesion proteins such as a decrease in a cell polarity protein, N-cadherin [49]. In this study, Cx32 overexpression resulted in a mesenchymal-like morphology that was accompanied by increased motility in MCF10A cells. The increase in migration of MCF10A cells due to Cx32 overexpression might be due to E-cadherin as E-cadherin levels were positively associated with migration in MCF10A cells [50]. Cx32 also altered the cell morphology in other cell types, where Cx32 knockout in hepatocytes resulted in stellate-like appearance compared to epithelioid morphology in WT cells [51], and Cx32 expression promoted neurite growth in C6 cells [52]. These observations support the effects of Cx32 on cell morphology and migration in a context-dependent manner.

Metastasis is the spread and colonization of cancer cells to a secondary organ that involves several steps in which cell-cell and cell-matrix interactions mediated by cell adhesion and gap junction proteins are quite essential [12]. One of the initial steps of metastasis includes the epithelial to mesenchymal transition (EMT) in which expression of epithelial markers such as E-cadherin, ZO-1 decreases, while that of mesenchymal markers including N-cadherin, Zeb2, vimentin and slug increases [53]. The involvement of connexins in EMT was shown for different isoforms [54]. For example, Cx43 overexpression increased the expression of E-cadherin and ZO-1 epithelial markers, while its downregulation increased N-cadherin mesenchymal marker expression in MDA-MB-231 cell lines, suggesting Cx43's role in the acquisition of an epithelial character in MDA-MB-231 cells [55]. The relation between Cx32 and EMT markers was also reported, where Cx32 expression in Huh7 hepatocellular carcinoma cells was positively correlated with E-cadherin expression and negatively associated with mesenchymal markers such as vimentin [56]. It was further suggested that Cx32

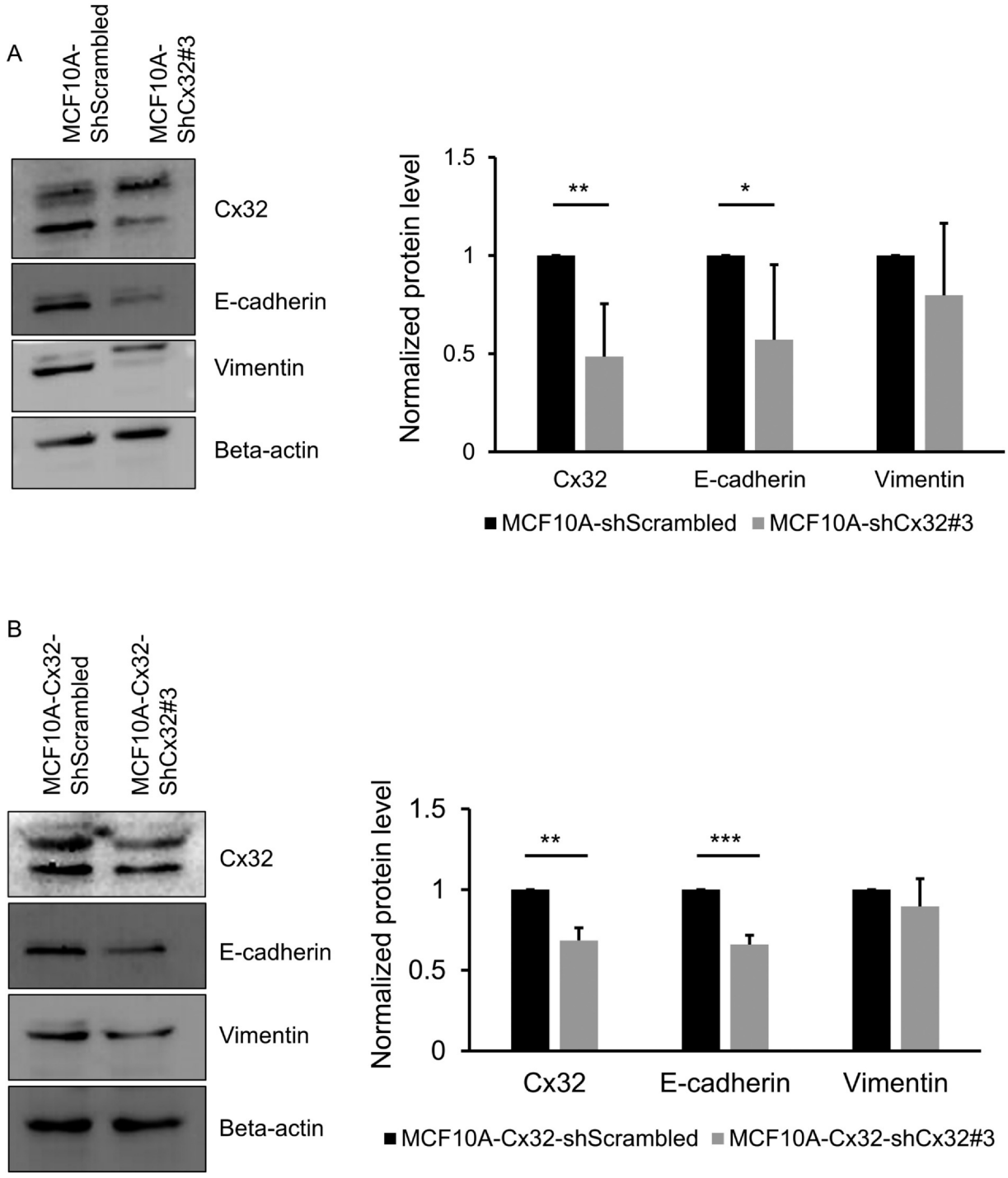

Fig. 7. Cx32 silencing decreased expression of E-cadherin in MCF10A cells. A) MCF10A and B) stable MCF10A-Cx32 cells were transiently transfected with scrambled and Cx32 shRNAs, E-cadherin and vimentin expression was compared between control and shCx32-transfected cells where reduction of Cx32 was associated with decrease in E-cadherin level (*$p < 0.05$, **$p < 0.01$ and *** $p < 0.001$; n = 3–5). All data are presented as mean ± S.D. by normalizing Cx32 values with respect to GFP controls.

downregulation reduced the chemotherapy toxicity via induction of EMT [56]. In parallel with these, low Cx32 expression was correlated with no or low E-cadherin expression and an increase in vimentin level in SMMC-7721 hepatocellular carcinoma cells along with morphological changes [57]. Here, we reported that Cx32 overexpression increased both E-cadherin and vimentin expression in MCF10A cells, while E-cadherin expression was reduced in MDA-MB-231 cells. The increased expression of both E-cadherin and vimentin in MCF10A cells upon Cx32 overexpression might indicate a transition state during EMT [58] and/or acquisition of a hybrid cell phenotype [59].

In summary, to the best of our knowledge, this is the first report investigating the effect of Cx32 in normal breast and breast cancer cells that suggests its tumor promoting effect in breast cancer. We also provided further support for the context-dependent effects of Cx32 in tumorigenesis as observed for other connexins.

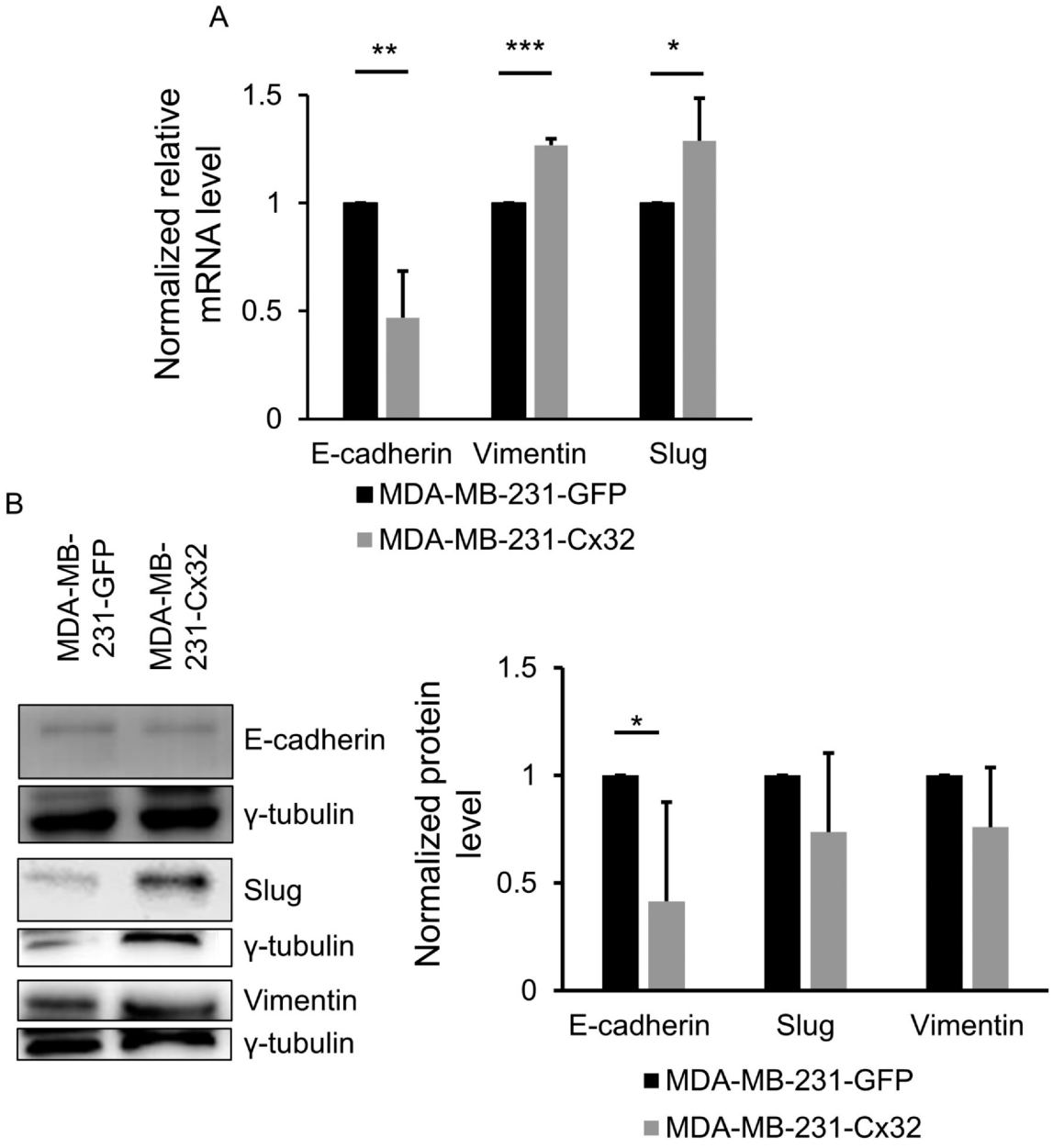

Fig. 8. Cx32 overexpression decreased E-cadherin mRNA and protein levels but increased vimentin and slug mRNA expression in MDA-MB-231 cells. Relative mRNA (A) and protein (B) levels of epithelial marker E-cadherin and mesenchymal marker vimentin, and slug in MDA-MB-231 cells suggested that MDA-MB-231 cells gained more mesenchymal properties (**$p < 0.01$, $n = 4$). All data are presented as mean ± S.D. by normalizing Cx32 values with respect to GFP controls.

CRediT authorship contribution statement

GM conceived the project; AA, YCU, ZV, FBT, SY, OYO and GM performed the experiments; GM, AA, YCU, OYO and EO designed the experiments; AA, YCU, SY, ZV, FBT, EO and GM analyzed the data; GM, AA and YCU wrote the manuscript; GM, EO, OYO and YCU revised the manuscript.

Declaration of competing interest

The authors declare that they have no known competing financial interests or personal relationships that could have appeared to influence the work reported in this paper.

Acknowledgement

We thank Dr. Steven Scherer from University of Pennsylvania, PA, USA for kindly providing the pIRES2-EGFP2-Cx32 vector. Main financial support by The Scientific and Technological Research Council of Turkey (Grant number 114Z874 to GM) is gratefully acknowledged. The Young Investigator Award by the Turkish Academy of Sciences to GM is also highly appreciated. We also would like to thank the Biotechnology and Bioengineering Research and Application Center, Izmir Institute of Technology staff for their expert technical help. Finally, proofreading by the Academic Writing Center, Izmir Institute of Technology was greatly appreciated.

References

[1] N. Harbeck, F. Penault-Llorca, J. Cortes, M. Gnant, N. Houssami, P. Poortmans, K. Ruddy, J. Tsang, F. Cardoso, Breast cancer, Nat Rev Dis Primers 5 (2019) 66.

[2] H. Yousefi, M. Maheronnaghsh, F. Molaei, L. Mashouri, A. Reza Aref, M. Momeny, S.K. Alahari, Long noncoding RNAs and exosomal lncRNAs: classification, and mechanisms in breast cancer metastasis and drug resistance, Oncogene 39 (2020) 953–974.
[3] L. Cronier, S. Crespin, P.O. Strale, N. Defamie, M. Mesnil, Gap junctions and cancer: new functions for an old story, Antioxid. Redox Signal. 11 (2009) 323–338.
[4] G. Mese, G. Richard, T.W. White, Gap junctions: basic structure and function, J Invest Dermatol 127 (2007) 2516–2524.
[5] M. Delmar, D.W. Laird, C.C. Naus, M.S. Nielsen, V.K. Verselis, T.W. White, Connexins and disease, Cold Spring Harb Perspect Biol 10 (2018) a029348.
[6] T. Aasen, E. Leithe, S.V. Graham, P. Kameritsch, M.D. Mayan, M. Mesnil, K. Pogoda, A. Tabernero, Connexins in cancer: bridging the gap to the clinic, Oncogene 38 (2019) 4429–4451.
[7] T. Aasen, M. Mesnil, C.C. Naus, P.D. Lampe, D.W. Laird, Gap junctions and cancer: communicating for 50 years, Nat. Rev. Cancer 17 (2017) 74.
[8] M. Srinivas, V.K. Verselis, T.W. White, Human diseases associated with connexin mutations, Biochim. Biophys. Acta Biomembr. 1860 (2018) 192–201.
[9] M.R. Calera, Z. Wang, R. Sanchez-Olea, D.L. Paul, M.M. Civan, D.A. Goodenough, Depression of intraocular pressure following inactivation of connexin43 in the nonpigmented epithelium of the ciliary body, Invest. Ophthalmol. Vis. Sci. 50 (2009) 2185–2193.
[10] J.A. El-Saghir, E.T. El-Habre, M.E. El-Sabban, R.S. Talhouk, Connexins: a junctional crossroad to breast cancer, Int J Dev Biol 55 (2011) 773–780.
[11] E. McLachlan, Q. Shao, D.W. Laird, Connexins and gap junctions in mammary gland development and breast cancer progression, J.Membr.Biol. 218 (2007) 107–121.
[12] D. Banerjee, Connexin's connection in breast cancer growth and progression, Int J Cell Biol 2016 (2016) 9025905.
[13] Q. Li, Y. Omori, Y. Nishikawa, T. Yoshioka, Y. Yamamoto, K. Enomoto, Cytoplasmic accumulation of connexin32 protein enhances motility and metastatic ability of human hepatoma cells in vitro and in vivo, Int. J. Cancer 121 (2007) 536–546.
[14] L. Kanczuga-Koda, S. Sulkowski, A. Lenczewski, M. Koda, A. Wincewicz, M. Baltaziak, M. Sulkowska, Increased expression of connexins 26 and 43 in lymph node metastases of breast cancer, J. Clin. Pathol. 59 (2006) 429–433.
[15] S.W. Lee, C. Tomasetto, D. Paul, K. Keyomarsi, R. Sager, Transcriptional down-regulation of gap-junction proteins blocks junctional communication in human mammary tumor cell lines, J. Cell Biol. 118 (1992) 1213–1221.
[16] E. McLachlan, Q. Shao, H.L. Wang, S. Langlois, D.W. Laird, Connexins act as tumor suppressors in three-dimensional mammary cell organoids by regulating differentiation and angiogenesis, Cancer Res. 66 (2006) 9886–9894.
[17] Y. Naoi, Y. Miyoshi, T. Taguchi, S.J. Kim, T. Arai, Y. Tamaki, S. Noguchi, Connexin26 expression is associated with lymphatic vessel invasion and poor prognosis in human breast cancer, Breast Cancer Res. Treat. 106 (2007) 11–17.
[18] I. Teleki, T. Krenacs, M.A. Szasz, J. Kulka, B. Wichmann, C. Leo, B. Papassotiropoulos, C. Riemenschnitter, H. Moch, Z. Varga, The potential prognostic value of connexin 26 and 46 expression in neoadjuvant-treated breast cancer, BMC Cancer 13 (2013) 50.
[19] C. Conklin, D. Huntsman, E. Yorida, N. Makretsov, D. Turbin, J.F. Bechberger, W.C. Sin, C.C. Naus, Tissue microarray analysis of connexin expression and its prognostic significance in human breast cancer, Cancer Lett. 255 (2007) 284–294.
[20] I. Teleki, A.M. Szasz, M.E. Maros, B. Gyorffy, J. Kulka, N. Meggyeshazi, G. Kiszner, P. Balla, A. Samu, T. Krenacs, Correlations of differentially expressed gap junction connexins Cx26, Cx30, Cx32, Cx43 and Cx46 with breast cancer progression and prognosis, PLoS One 9 (2014) e112541.
[21] N.M. Kumar, N.B. Gilula, Cloning and characterization of human and rat liver cDNAs coding for a gap junction protein, J. Cell Biol. 103 (1986) 767–776.
[22] J. Qin, M. Chang, S. Wang, Z. Liu, W. Zhu, Y. Wang, F. Yan, J. Li, B. Zhang, G. Dou, J. Liu, X. Pei, Y. Wang, Connexin 32-mediated cell-cell communication is essential for hepatic differentiation from human embryonic stem cells, Sci. Rep. 6 (2016) 37388.
[23] H. Pei, C. Zhai, H. Li, F. Yan, J. Qin, H. Yuan, R. Zhang, S. Wang, W. Zhang, M. Chang, Y. Wang, X. Pei, Connexin 32 and connexin 43 are involved in lineage restriction of hepatic progenitor cells to hepatocytes, Stem Cell Res Ther 8 (2017) 252.
[24] I.M. Neuhaus, L. Bone, S. Wang, V. Ionasescu, R. Werner, The human connexin32 gene is transcribed from two tissue-specific promoters, Biosci. Rep. 16 (1996) 239–248.
[25] B.A. Cisterna, P. Arroyo, C. Puebla, Role of connexin-based gap junction channels in communication of myelin sheath in Schwann cells, Front. Cell. Neurosci. 13 (2019) 69.
[26] J. Bergoffen, S.S. Scherer, S. Wang, M.O. Scott, L.J. Bone, D.L. Paul, K. Chen, M.W. Lensch, P.F. Chance, K.H. Fischbeck, Connexin mutations in X-linked Charcot-Marie-tooth disease, Science 262 (1993) 2039–2042.
[27] A. Temme, O. Traub, K. Willecke, Downregulation of connexin32 protein and gap-junctional intercellular communication by cytokine-mediated acute-phase response in immortalized mouse hepatocytes, Cell Tissue Res. 294 (1998) 345–350.
[28] T.J. King, P.D. Lampe, The gap junction protein connexin32 is a mouse lung tumor suppressor, Cancer Res. 64 (2004) 7191–7196.
[29] G.O. Edwards, S. Jondhale, T. Chen, J.K. Chipman, A quantitative inverse relationship between connexin32 expression and cell proliferation in a rat hepatoma cell line, Toxicology 253 (2008) 46–52.
[30] Y. Xiang, Q. Wang, Y. Guo, H. Ge, Y. Fu, X. Wang, L. Tao, Cx32 exerts anti-apoptotic and pro-tumor effects via the epidermal growth factor receptor pathway in hepatocellular carcinoma, J. Exp. Clin. Cancer Res. 38 (2019) 145.
[31] R.S. Talhouk, R.C. Elble, R. Bassam, M. Daher, A. Sfeir, L.A. Mosleh, H. El-Khoury, S. Hamoui, B.U. Pauli, M.E. El-Sabban, Developmental expression patterns and regulation of connexins in the mouse mammary gland: expression of connexin30 in lactogenesis, Cell Tissue Res. 319 (2005) 49–59.
[32] L. Kanczuga-Koda, M. Sulkowska, M. Koda, R. Rutkowski, S. Sulkowski, Increased expression of gap junction protein—connexin 32 in lymph node metastases of human ductal breast cancer, Folia Histochem. Cytobiol. 45 (Suppl. 1) (2007) S175–S180.
[33] T. Zengin, B. Ekinci, C. Kucukkose, O. Yalcin-Ozuysal, IRF6 is involved in the regulation of cell proliferation and transformation in MCF10A cells downstream of notch signaling, PLoS One 10 (2015) e0132757.
[34] H. Aypek, V. Bay, G. Mese, Altered cellular localization and hemichannel activities of KID syndrome associated connexin26 I30N and D50Y mutations, BMC Cell Biol. 17 (2016) 5.
[35] R.P. Huang, Y. Fan, M.Z. Hossain, A. Peng, Z.L. Zeng, A.L. Boynton, Reversion of the neoplastic phenotype of human glioblastoma cells by connexin 43 (cx43), Cancer Res. 58 (1998) 5089–5096.
[36] M. Ilhan, C. Kucukkose, E. Efe, Z.E. Gunyuz, B. Firatligil, H. Dogan, M. Ozuysal, O. Yalcin-Ozuysal, Pro-metastatic functions of notch signaling is mediated by CYR61 in breast cells, Eur. J. Cell Biol. 99 (2020) 151070.
[37] J.M. Burt, T.K. Nelson, A.M. Simon, J.S. Fang, Connexin 37 profoundly slows cell cycle progression in rat insulinoma cells, Am J Physiol Cell Physiol 295 (2008) C1103–C1112.
[38] T. Uynuk-Ool, M. Rothdiener, B. Walters, M. Hegemann, J. Palm, P. Nguyen, T. Seeger, U. Stockle, J.P. Stegemann, W.K. Aicher, B. Kurz, M.L. Hart, G. Klein, B. Rolauffs, The geometrical shape of mesenchymal stromal cells measured by quantitative shape descriptors is determined by the stiffness of the biomaterial and by cyclic tensile forces, J. Tissue Eng. Regen. Med. 11 (2017) 3508–3522.
[39] M. Kotini, E.H. Barriga, J. Leslie, M. Gentzel, V. Rauschenberger, A. Schambony, R. Mayor, Gap junction protein Connexin-43 is a direct transcriptional regulator of N-cadherin in vivo, Nat. Commun. 9 (2018) 3846.
[40] K. Stoletov, J. Strnadel, E. Zardouzian, M. Momiyama, F.D. Park, J.A. Kelber, D.P. Pizzo, R. Hoffman, S.R. VandenBerg, R.L. Klemke, Role of connexins in metastatic breast cancer and melanoma brain colonization, J. Cell Sci. 126 (2013) 904–913.
[41] Y.W. Zhang, K. Nakayama, I. Morita, A novel route for connexin 43 to inhibit cell proliferation: negative regulation of S-phase kinase-associated protein (Skp 2), Cancer Res. 63 (2003) 1623–1630.
[42] Q. Shi, J.X. Jiang, Connexin arrests the cell cycle through cytosolic retention of an E3 ligase, Mol Cell Oncol 3 (2016) e1132119.
[43] H. Jee, S.H. Lee, J.W. Park, B.R. Lee, K.T. Nam, D.Y. Kim, Connexin32 inhibits gastric carcinogenesis through cell cycle arrest and altered expression of p21Cip1 and p27Kip1, BMB Rep. 46 (2013) 25–30.
[44] C. Cina, K. Maass, M. Theis, K. Willecke, J.F. Bechberger, C.C. Naus, Involvement of the cytoplasmic C-terminal domain of connexin43 in neuronal migration, J. Neurosci. 29 (2009) 2009–2021.
[45] D.C. Bates, W.C. Sin, Q. Aftab, C.C. Naus, Connexin43 enhances glioma invasion by a mechanism involving the carboxy terminus, Glia 55 (2007) 1554–1564.
[46] M. Kotini, R. Mayor, Connexins in migration during development and cancer, Dev. Biol. 401 (2015) 143–151.
[47] X. Xu, R. Francis, C.J. Wei, K.L. Linask, C.W. Lo, Connexin 43-mediated modulation of polarized cell movement and the directional migration of cardiac neural crest cells, Development 133 (2006) 3629–3639.
[48] H. Qin, Q. Shao, H. Curtis, J. Galipeau, D.J. Belliveau, T. Wang, M.A. Alaoui-Jamali, D.W. Laird, Retroviral delivery of connexin genes to human breast tumor cells inhibits in vivo tumor growth by a mechanism that is independent of significant gap junctional intercellular communication, J. Biol. Chem. 277 (2002) 29132–29138.
[49] K.J. Simpson, L.M. Selfors, J. Bui, A. Reynolds, D. Leake, A. Khvorova, J.S. Brugge, Identification of genes that regulate epithelial cell migration using an siRNA screening approach, Nat. Cell Biol. 10 (2008) 1027–1038.
[50] A. Chen, H. Beetham, M.A. Black, R. Priya, B.J. Telford, J. Guest, G.A. Wiggins, T.D. Godwin, A.S. Yap, P.J. Guilford, E-cadherin loss alters cytoskeletal organization and adhesion in non-malignant breast cells but is insufficient to induce an epithelial-mesenchymal transition, BMC Cancer 14 (2014) 552.
[51] T. Kojima, D.C. Spray, Y. Kokai, H. Chiba, Y. Mochizuki, N. Sawada, Cx32 formation and/or Cx32-mediated intercellular communication induces expression and function of tight junctions in hepatocytic cell line, Exp. Cell Res. 276 (2002) 40–51.
[52] M.L. Cotrina, J.H. Lin, J.C. Lopez-Garcia, C.C. Naus, M. Nedergaard, ATP-mediated glia signaling, J. Neurosci. 20 (2000) 2835–2844.
[53] R. Kalluri, R.A. Weinberg, The basics of epithelial-mesenchymal transition, J. Clin. Invest. 119 (2009) 1420–1428.
[54] J.I. Wu, L.H. Wang, Emerging roles of gap junction proteins connexins in cancer metastasis, chemoresistance and clinical application, J. Biomed. Sci. 26 (2019) 8.
[55] J.M. Kazan, J. El-Saghir, J. Saliba, A. Shaito, N. Jalaleddine, L. El-Hajjar, S. Al-Ghadban, L. Yehia, K. Zibara, M. El-Sabban, Cx43 expression correlates with breast cancer metastasis in MDA-MB-231 cells in vitro, in a mouse xenograft model and in human breast cancer tissues, Cancers (Basel) 11 (2019).
[56] Y. Yang, J.H. Yao, Q.Y. Du, Y.C. Zhou, T.J. Yao, Q. Wu, J. Liu, Y.R. Ou, Connexin 32 downregulation is critical for chemoresistance in oxaliplatin-resistant HCC cells associated with EMT, Cancer Manag. Res. 11 (2019) 5133–5146.
[57] Y. Yang, N. Zhang, J. Zhu, X.T. Hong, H. Liu, Y.R. Ou, F. Su, R. Wang, Y.M. Li, Q. Wu, Downregulated connexin32 promotes EMT through the Wnt/beta-catenin pathway by targeting snail expression in hepatocellular carcinoma, Int. J. Oncol. 50 (2017) 1977–1988.
[58] M.A. Nieto, R.Y. Huang, R.A. Jackson, J.P. Thiery, Emt: 2016, Cell 166 (2016) 21–45.
[59] H.J. Hugo, N. Gunasinghe, B.G. Hollier, T. Tanaka, T. Blick, A. Toh, P. Hill, C. Gilles, M. Waltham, E.W. Thompson, Epithelial requirement for in vitro proliferation and xenograft growth and metastasis of MDA-MB-468 human breast cancer cells: oncogenic rather than tumor-suppressive role of E-cadherin, Breast Cancer Res. 19 (2017) 86.